CHAPTER 19

COLLIMATED IRRADIATION AND TRANSIENT PHENOMENA

19.1 INTRODUCTION

In recent years, there has been increasing interest in the analysis of radiative transfer in multidimensional absorbing, emitting, and scattering media with collimated irradiation. By collimated irradiation we mean external radiation that penetrates from the outside into a participating medium (as opposed to emission from a bounding surface), with all light waves being parallel to one another (or approximately so). Typical examples include solar radiation through the atmosphere and into the ocean, laser irradiation of particles or liquids, and so on. With the advent of short-pulsed lasers with pulse durations measured in pico- or even femtoseconds, transient radiation effects have also become of interest. Since, in engineering applications, virtually all transient radiation effects are due to short-pulsed lasers, these two topics are treated jointly in the present chapter. By collimated irradiation we mean that the intensity incident on a surface dA at location $\mathbf{r}_w$ on the bounding surface of the medium, as shown in Fig. 19-1, may be written as

$$\begin{aligned} I_{ow}(\mathbf{r}_w, \hat{\mathbf{s}}) &= q_o(\mathbf{r}_w)\, \delta\left[\hat{\mathbf{s}} - \hat{\mathbf{s}}_o(\mathbf{r}_w)\right] \\ &= q_o(\mathbf{r}_w)\, \delta\left[\mu - \mu_o(\mathbf{r}_w)\right] \delta[\psi - \psi_o(\mathbf{r}_w)], \end{aligned} \tag{19.1}$$

where δ is the Dirac-delta function, which is here defined as[1]

$$\delta(x) = \begin{cases} 0, & |x| > \epsilon, \\ \lim\limits_{\epsilon \to 0} \dfrac{1}{2\epsilon}, & |x| < \epsilon, \end{cases} \tag{19.2a}$$

$$\int_{4\pi} f(\hat{\mathbf{s}})\, \delta(\hat{\mathbf{s}} - \hat{\mathbf{s}}_o)\, d\Omega = \int_0^{2\pi} \int_{-1}^{+1} f(\mu, \psi)\, \delta(\mu - \mu_o)\, \delta(\psi - \psi_o)\, d\mu\, d\psi = f(\mu_o, \psi_o), \tag{19.2b}$$

and

$$\hat{\mathbf{s}}_o = \cos\theta_o \hat{\mathbf{n}} + \sin\theta_o(\cos\psi_o \hat{\mathbf{t}}_1 + \sin\psi_o \hat{\mathbf{t}}_2), \qquad \mu_o = \cos\theta_o, \tag{19.3}$$

is the direction from which the collimated radiation impinges onto the medium (with $\hat{\mathbf{n}}$ the surface normal pointing into the medium and $\hat{\mathbf{t}}_1$ and $\hat{\mathbf{t}}_2$ two orthogonal unit vectors lying on the

[1] For a definition of the standard, one-dimensional Dirac-delta function see equation (11.99) in Section 11.9.

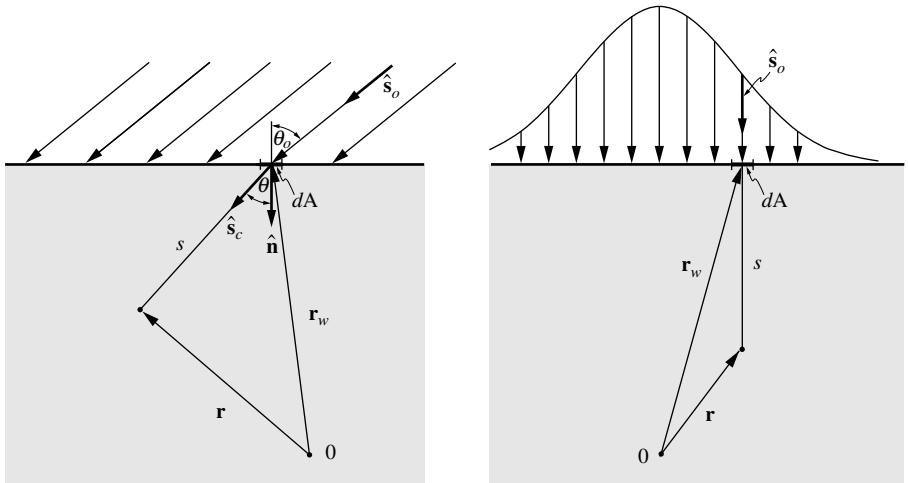

FIGURE 19-1
Collimated irradiation impinging on an arbitrary surface: (*a*) solar irradiation, (*b*) laser irradiation.

boundary surface). Equation (19.1) implies that the incident intensity is zero for all directions except for $\hat{\mathbf{s}}_o$, where it is infinitely large. The total heat flux within the collimated irradiation is determined from

$$\mathbf{q}_o = \int_{4\pi} I_{ow}(\hat{\mathbf{s}})\,\hat{\mathbf{s}}\,d\Omega = q_o \int_{4\pi} \hat{\mathbf{s}}\,\delta(\hat{\mathbf{s}} - \hat{\mathbf{s}}_o)\,d\Omega = q_o \hat{\mathbf{s}}_o, \tag{19.4}$$

that is, q_o is the total radiative heat flux of the collimated irradiation through a surface normal to the rays. The component penetrating into the medium is then

$$\mathbf{q}_c = [1 - \rho(\mathbf{r}_w, \hat{\mathbf{s}}_o)]\, q_o \hat{\mathbf{s}}_c, \tag{19.5}$$

where ρ is the reflectance of the interface in the direction of $\hat{\mathbf{s}}_o$. Since the irradiation penetrating into the medium may be refracted, the unit direction vector inside the medium is denoted as $\hat{\mathbf{s}}_c$, which may be different from $\hat{\mathbf{s}}_o$. As indicated in the above expressions the magnitude of the irradiation q_o, as well as the direction of irradiation, $\hat{\mathbf{s}}_o$, may vary over the surface of the enclosure, while the reflectance of the surface may vary with position and direction.

In a strictly mathematical sense equation (19.1) introduces nothing new: Collimated irradiation could simply be treated as "strongly directional emission." However, the discontinuity of intensity with direction causes problems with analytical as well as numerical solution techniques, thus warranting a separate approach for this type of problem.

Most earlier works on collimated radiation dealt with solar radiation and other atmospheric or astrophysical applications. They are, therefore, generally limited to one-dimensional cases with uniform irradiation of a planar medium. For this simple case, some exact and approximate solutions have been given by Irvine [1], who used the Henyey–Greenstein phase function, a scattering phase function that adequately approximates the anisotropic scattering behavior of a large number of media [2], as given by equation (12.95). The identical problem for Rayleigh scattering was treated by Kubo [3] without, however, reporting any results. Armaly and El-Baz [4] found some approximate solutions for isotropic scattering in a finite-thickness slab using the kernel approximation. Their application was in the area of solar collectors. A similar problem was treated by Houf and Incropera [5], who investigated different approximate techniques for solar irradiation of aqueous media.

Only with the advent of the laser as a research and manufacturing tool has nonsolar collimated radiation received some research attention. Smith [6] investigated the case of a uniform strip of collimated radiation incident on a semi-infinite medium. The resulting two-dimensional

integral equation was reduced to one-dimensional form using Fourier transforms. Hunt [7] investigated the effect of a cylindrical collimated beam impinging upon a finite layer. A solution was found for the basic case of Bessel-function varying intensity using Green's functions. The first ones to apply this theory to laser radiation appear to be Beckett and coworkers [8], who investigated numerically the effect of a cylindrical beam with Gaussian variation penetrating through a finite layer. They showed how a diagnostic laser beam can be used to deduce radiative properties of an optically thick slab, such as single-scattering albedo, extinction, and absorption coefficients. Finally, a number of papers by Crosbie and coworkers [9–12] dealt with exact solutions to the general two-dimensional problem of collimated radiation impinging onto an absorbing–scattering layer. First, they treated collimated strip sources irradiating a semi-infinite body [9]; later, they discussed cylindrical beams falling on a semi-infinite body [10, 11]. Collimated irradiation onto a rectangular medium was investigated by Crosbie and Schrenker [12] for isotropic scattering, while Kim and Lee [13] demonstrated the accuracy of the high-order discrete ordinates method by applying it to the same problem with anisotropic scattering. The exact solutions may be used as benchmarks for evaluation of approximate methods and may be necessary in cases where the requirement for highly accurate results justifies going through the trouble usually associated with these methods. In the area of heat transfer, however, approximate solutions often result in acceptable predictions for most practical situations.

Recently, some more advanced problems have also become of interest. Tan and coworkers considered combined conduction and radiative laser heating of glass [14], while Lacroix and colleagues [15] and Xu and Song [16, 17] applied the discrete ordinates method to analyze the interaction of a laser beam with the plume or plasma generated by the laser. El Ammouri *et al.* [18] showed how laser beam fluctuations, caused by temperature fluctuations, can be employed as a tool to measure turbulence levels. Along the same line Ben-Abdallah [19] and coworkers analyzed the curved beam path that a laser traverses in a gas with varying refractive index.

Lasers with ultra-short pulse lengths are utilized heavily in the emerging field of nanotechnology and also in biomedical engineering [20]. The radiative fields generated by such short-pulsed lasers may differ from those discussed in this book in two important aspects: (1) since light travels only 300 μm during a time span of 1 ps, transient effects must be accounted for, and (2) packing a fixed amount of energy into a pulse of extremely short duration leads to temporally extreme intensities. The former requires consideration of the transient term in the RTE, equation (10.20), and has been investigated by a number of researchers [21–32]. At very high intensities, many molecules are promoted to excited levels, which have different absorption behavior, making the absorption coefficient a function of intensity; this is known as *saturable absorption* [33]. Depending on the relative magnitude of absorption cross-sections, this may lead to *bleaching* (absorption coefficient decreases with intensity) or *darkening* (absorption coefficient increases with intensity) [34]. In addition, at very high intensities molecules may absorb more than a single photon at the same time, raising the molecule to an excited electronic state. This is known as *multiphoton absorption* [35–37]. If the total absorbed photon energy is high enough this, in turn, may lead to ionization or dissociation, which is known as *photolysis*. Several photochemical and photothermal models have been developed to describe short-pulse laser ablation of materials [38–41]. In biomedical engineering short-pulsed lasers are seen as promising tools for optical imaging (of tumors, etc.) [24, 42, 43] and for minimally invasive surgery (such as ablation of tumors) [44].

In this chapter we shall describe how problems involving radiative transfer in an absorbing, emitting, and anisotropically scattering medium of arbitrary geometry exposed to arbitrary collimated irradiation[2] are dealt with by separating the collimated radiation (as it travels through the medium) from the rest of the radiation field. The problem is thus reduced to one without

[2]We shall limit our discussion to unpolarized irradiation, even though laser sources are always polarized (circularly or linearly). Polarization together with specular reflections may result in a number of interesting effects, for example, in the area of laser processing of materials [45, 46].

collimated irradiation, but with a modified radiation source term (now including a source due to the scattered part of the collimated irradiation). We shall see that it is possible to incorporate collimated irradiation readily into well-known approximate methods such as the P_1-approximation. Because of its emerging importance, the chapter also includes a very brief section on transient effects during short-pulsed laser irradiation.

19.2 REDUCTION OF THE PROBLEM

The equation of transfer for an absorbing, emitting, and anisotropically scattering medium is given by equation (10.18) as

$$\hat{\mathbf{s}} \cdot \nabla I(\mathbf{r}, \hat{\mathbf{s}}) = \kappa I_b(\mathbf{r}) - \beta I(\mathbf{r}, \hat{\mathbf{s}}) + \frac{\sigma_s}{4\pi} \int_{4\pi} I(\mathbf{r}, \hat{\mathbf{s}}') \, \Phi(\hat{\mathbf{s}}, \hat{\mathbf{s}}') \, d\Omega'. \tag{19.6}$$

As usual, the lack of a spectral subscript implies that we deal either with spectral intensity or with a gray medium. We shall limit ourselves here to media with diffusely emitting and reflecting boundaries. Then the boundary condition for equation (19.6) is, for any location $\mathbf{r}_w$ on the surface,

$$I(\mathbf{r}_w, \hat{\mathbf{s}}) = [1 - \rho(\mathbf{r}_w)] \, I_{ow}(\mathbf{r}_w, \hat{\mathbf{s}}) + \epsilon(\mathbf{r}_w) I_{bw}(\mathbf{r}_w) + \frac{\rho(\mathbf{r}_w)}{\pi} \int_{\hat{\mathbf{n}} \cdot \hat{\mathbf{s}}' < 0} I(\mathbf{r}_w, \hat{\mathbf{s}}') \, |\hat{\mathbf{n}} \cdot \hat{\mathbf{s}}'| \, d\Omega'. \tag{19.7}$$

Here the first term on the right-hand side represents penetration of collimated radiation, the second term describes emission from the surrounding medium, and the last term is due to diffuse reflection at the interface. This distribution is shown schematically in Fig. 19-2*a*. Since we assume here diffuse emission and reflection and are looking at spectral relations or a gray medium, we also have $\epsilon = 1 - \rho$.

We now separate the intensity within the medium into two parts: (*i*) the remnant of the collimated beam after partial extinction, by absorption and scattering, along its path, and (*ii*) a fairly diffuse part, which is the result of emission from the boundaries, emission from within the medium, and the radiation scattered away from the collimated irradiation. Thus, we set

$$I(\mathbf{r}, \hat{\mathbf{s}}) = I_c(\mathbf{r}, \hat{\mathbf{s}}) + I_d(\mathbf{r}, \hat{\mathbf{s}}), \tag{19.8}$$

where the collimated remnant of the irradiation obeys the equation of transfer

$$\hat{\mathbf{s}} \cdot \nabla I_c(\mathbf{r}, \hat{\mathbf{s}}) = -\beta I_c(\mathbf{r}, \hat{\mathbf{s}}), \tag{19.9}$$

subject to the boundary condition

$$I_c(\mathbf{r}_w, \hat{\mathbf{s}}) = [1 - \rho(\mathbf{r}_w)] \, q_o(\mathbf{r}_w) \, \delta [\hat{\mathbf{s}} - \hat{\mathbf{s}}_c(\mathbf{r}_w)] \, . \tag{19.10}$$

Equations (19.9) and (19.10) are readily solved as[3]

$$I_c(\mathbf{r}, \hat{\mathbf{s}}) = [1 - \rho(\mathbf{r}_w)] \, q_o(\mathbf{r}_w) \, \delta [\hat{\mathbf{s}} - \hat{\mathbf{s}}_c(\mathbf{r}_w)] \, e^{-\tau_c}, \tag{19.11}$$

where $\tau_c = \int_0^s \beta \, ds'$ and $s = |\mathbf{r} - \mathbf{r}_w|$ as indicated in Fig. 19-2*b*. Substituting equations (19.8) and (19.9) into equation (19.6) gives the equation of transfer for the noncollimated radiation as

$$\frac{1}{\beta} \hat{\mathbf{s}} \cdot \nabla I_d(\mathbf{r}, \hat{\mathbf{s}}) = \hat{\mathbf{s}} \cdot \nabla_\tau I_d(\mathbf{r}, \hat{\mathbf{s}}) = -I_d(\mathbf{r}, \hat{\mathbf{s}}) + \frac{\omega}{4\pi} \int_{4\pi} I_d(\mathbf{r}, \hat{\mathbf{s}}') \, \Phi(\hat{\mathbf{s}}, \hat{\mathbf{s}}') \, d\Omega' + (1 - \omega) \, I_b(\mathbf{r}) + \omega S_c(\mathbf{r}, \hat{\mathbf{s}}), \tag{19.12}$$

[3]For simplicity of notation, equation (19.11) and the following development assumes collimated radiation from a single direction; if multiple collimated sources are present I_c is found by summation.

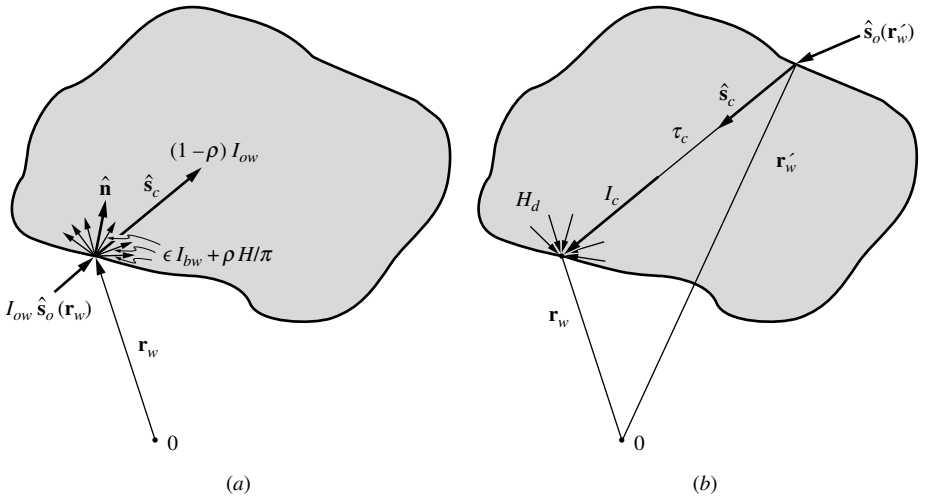

FIGURE 19-2
Radiative intensity at the surface of an enclosure with collimated irradiation: (*a*) outgoing intensity, (*b*) incoming intensity.

where the abbreviation

$$S_c(\mathbf{r}, \hat{\mathbf{s}}) \equiv \frac{1}{4\pi} \int_{4\pi} I_c(\mathbf{r}, \hat{\mathbf{s}}')\, \Phi(\hat{\mathbf{s}}, \hat{\mathbf{s}}')\, d\Omega' = \frac{1}{4\pi} \left[1 - \rho(\mathbf{r}_w)\right] q_o(\mathbf{r}_w)\, e^{-\tau_c} \Phi(\hat{\mathbf{s}}, \hat{\mathbf{s}}_c) \tag{19.13}$$

has been introduced and ∇_τ again implies that the gradient is to be taken with respect to nondimensional optical coordinates. Thus, S_c is a radiative source term resulting from radiation scattered away from the collimated beam; it behaves similarly to I_b, although this "emission" may not be isotropic (in the case of anisotropic scattering). Similarly, substituting equations (19.8) and (19.10) into equation (19.7) gives the boundary condition for equation (19.12) as

$$I_d(\mathbf{r}_w, \hat{\mathbf{s}}) = \epsilon I_{bw}(\mathbf{r}_w) + \frac{\rho(\mathbf{r}_w)}{\pi} \left[H_c(\mathbf{r}_w) + \int_{\hat{\mathbf{n}} \cdot \hat{\mathbf{s}}' < 0} I_d(\mathbf{r}_w, \hat{\mathbf{s}}')\, |\hat{\mathbf{n}} \cdot \hat{\mathbf{s}}'|\, d\Omega' \right], \tag{19.14}$$

where

$$H_c(\mathbf{r}_w) \equiv \int_{\hat{\mathbf{n}} \cdot \hat{\mathbf{s}}' < 0} I_c(\mathbf{r}_w, \hat{\mathbf{s}}')\, |\hat{\mathbf{n}} \cdot \hat{\mathbf{s}}'|\, d\Omega' = \left[1 - \rho(\mathbf{r}_w')\right] q_o(\mathbf{r}_w') |\hat{\mathbf{n}} \cdot \hat{\mathbf{s}}_c'|\, e^{-\tau_c} \tag{19.15}$$

is a surface irradiation term due to the collimated beam, and its diffuse reflection results in an additional surface source similar to I_{bw}. In this expression $\mathbf{r}_w'$ is the location at which the collimated beam enters the medium with a direction of $\hat{\mathbf{s}}_c'$, and $\mathbf{r}_w$ is the next point on the enclosure surface that the beam hits after traversing through the medium, as shown in Fig. 19-2*b*.

Inspection of equations (19.12) and (19.14) shows that, for isotropic scattering, the intensity field for I_d is readily determined from standard methods, after replacing I_b within the medium by $I_b + (\sigma_s/\kappa) S_c$, and I_{bw} at the enclosure surface by $I_{bw} + (\rho/\epsilon) H_c/\pi$. In the case of anisotropic scattering the emission term S_c becomes direction-dependent, which may necessitate slight changes in the solution procedure.

Example 19.1. Consider a plane-parallel slab of an absorbing and isotropically scattering medium as shown in Fig. 19-3. The medium is gray (with absorption coefficient κ, scattering coefficient σ_s, and a refractive index of $n = 1$), cold (i.e., essentially nonemitting) and of constant thickness L. At the top ($z = 0$) the layer is bounded by a nonparticipating gas ($n = 1$) and is exposed to solar radiation impinging at θ_o off-normal. At the bottom of the layer ($z = L$) the medium is bounded by a cold black surface. Determine radiative heat flux (and its divergence) as functions of depth.

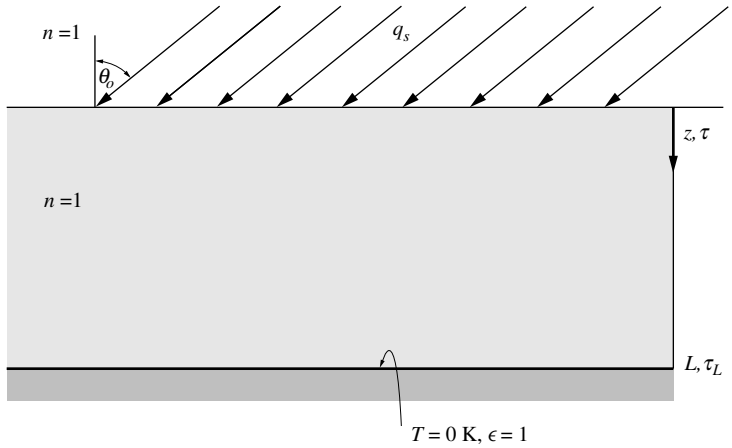

FIGURE 19-3
Geometry for Example 19.1.

Solution
Since both media have the same index of refraction the interface reflectivity is $\rho = 0$ and $\hat{\mathbf{s}}_c = \hat{\mathbf{s}}_o$; from equation (19.11) we find immediately

$$I_c(\tau, \hat{\mathbf{s}}) = q_s e^{-\tau/\mu_o} \delta(\hat{\mathbf{s}} - \hat{\mathbf{s}}_o),$$

as well as

$$S_c(\tau) = \frac{G_c}{4\pi}(\tau) = \frac{q_s}{4\pi} e^{-\tau/\mu_o},$$

$$\mathbf{q}_c(\tau) = q_s e^{-\tau/\mu_o} \hat{\mathbf{s}}_o.$$

The heat flux vector due to collimated irradiation has two components, one in the direction of τ, the other in a direction normal to it (in the plane formed by $\hat{\mathbf{s}}_o$ and the surface normal). Thus, the overall problem is two-dimensional. However, inspection of the source term in equation (19.12) shows that the source is isotropic, as are the boundary conditions for equation (19.12). Therefore, I_d can depend only on distance perpendicular to the surfaces, τ, and on polar angle. Thus,

$$\mu \frac{dI_d}{d\tau} + I_d = \omega \left[\frac{1}{4\pi} \int_{4\pi} I_d \, d\Omega' + S_c \right] = \frac{\omega}{4\pi} \left[G_d(\tau) + G_c(\tau) \right].$$

The boundary conditions are

$$\tau = 0: \qquad I(0, \hat{\mathbf{s}}) = q_s \delta(\hat{\mathbf{s}} - \hat{\mathbf{s}}_o), \qquad 0 \le \theta < \frac{\pi}{2},$$

$$\tau = \tau_L: \qquad I(\tau_L, \hat{\mathbf{s}}) = 0, \qquad \frac{\pi}{2} < \theta \le \pi,$$

or, after subtracting the collimated component,

$$\tau = 0: \qquad I_d(0, \mu) = 0, \qquad 0 < \mu \le 1,$$

$$\tau = \tau_L: \qquad I_d(\tau, \mu) = 0, \qquad -1 \le \mu < 0.$$

Therefore, with $S = (\omega/4\pi)(G_d + G_c)$, the solution for I_d is, from equation (14.21),

$$G_d(\tau) = 2\pi \int_0^{\tau_L} \frac{\omega}{4\pi} (G_d + G_c)(\tau') E_1(|\tau - \tau'|) \, d\tau'.$$

In nondimensional form, with $\Phi(\tau) = (G_d + G_c)/q_s$, this expression becomes

$$\Phi(\tau) - e^{-\tau/\mu_o} = \frac{\omega}{2} \int_0^{\tau_L} \Phi(\tau') E_1(|\tau - \tau'|) \, d\tau'.$$

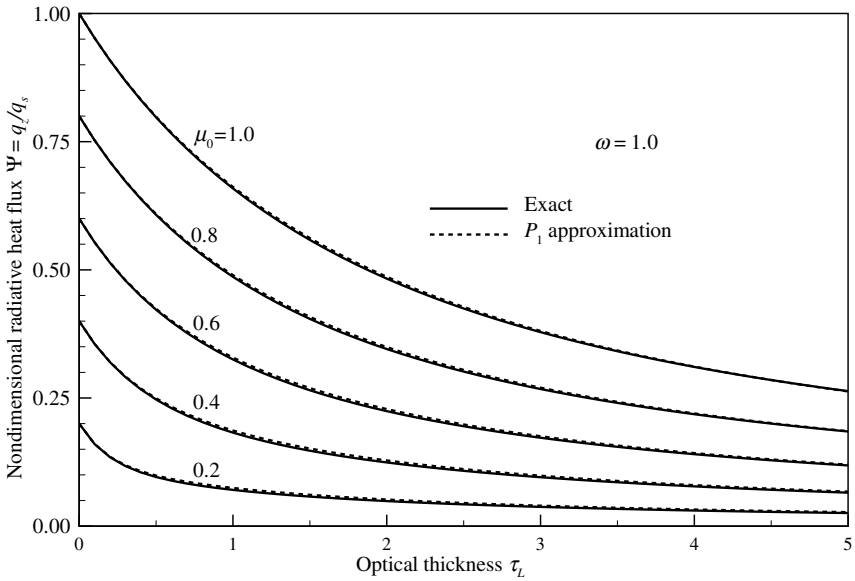

FIGURE 19-4
Nondimensional radiative heat flux in a purely scattering layer with collimated irradiation.

This integral equation must be solved numerically in the same fashion as equation (14.43). Once the function $\Phi(\tau)$ has been determined, the diffuse component of the heat flux is found from equation (14.22) as

$$\mathbf{q}_d(\tau) = q_d(\tau)\,\hat{\mathbf{k}} = 2\pi \int_{-1}^{1} I_d \mu \, d\mu \, \hat{\mathbf{k}},$$

$$q_d(\tau) = 2\pi \left\{ \int_0^{\tau} \frac{\omega}{4\pi}(G_d + G_c)(\tau')E_2(\tau - \tau')\,d\tau' - \int_{\tau}^{\tau_L} \frac{\omega}{4\pi}(G_d + G_c)(\tau')E_2(\tau' - \tau)\,d\tau' \right\}.$$

Finally, the total heat flux in the τ-direction, on a nondimensional basis, is

$$\Psi = \frac{\mathbf{q}_c \cdot \hat{\mathbf{k}} + q_d}{q_s} = \mu_o\, e^{-\tau/\mu_o} + \frac{\omega}{2}\left[\int_0^{\tau} \Phi(\tau')E_2(\tau - \tau')\,d\tau' - \int_{\tau}^{\tau_L} \Phi(\tau')E_2(\tau' - \tau)\,d\tau' \right].$$

The divergence of the radiative heat flux is found from equation (10.59) as

$$\nabla_\tau \cdot \mathbf{q} = (1 - \omega)(4\pi I_b - G) = -(1 - \omega)(G_c + G_d),$$

or in nondimensional form

$$\frac{1}{q_s}\nabla_\tau \cdot \mathbf{q} = -(1 - \omega)\Phi.$$

Some results for a purely scattering medium ($\omega = 1$) are shown in Fig. 19-4. For that case we find $\nabla \cdot \mathbf{q} = 0$ and, since the tangential component of $\mathbf{q}_c$ does not depend on tangential direction, $\mathbf{q} \cdot \hat{\mathbf{k}} =$ const and $\Psi =$ const. Thus, evaluating the heat flux at $\tau = 0$, we get

$$\Psi(\omega = 1) = \mu_o - \frac{1}{2}\int_0^{\tau_L} \Phi(\tau')E_2(\tau')\,d\tau'.$$

19.3 THE MODIFIED P_1-APPROXIMATION WITH COLLIMATED IRRADIATION

As for problems without collimated irradiation, exact or approximate solutions to equation (19.12), together with its boundary condition (19.14), may be found using a variety of different methods.

As an illustration we will show here how the P_1-approximation may be applied to problems with collimated irradiation, following the development of Modest and Tabanfar [47]. The P_1 or *differential approximation* is simple to use (requiring only the solution of an elliptic differential equation) and powerful (applicable to multidimensional geometries, as well as to anisotropic scattering). Unfortunately, the fact that the P_1-approximation is accurate only for smoothly varying (with direction) intensity fields makes the method particularly unsuitable for problems with collimated irradiation. However, once the collimated intensity, I_c, has been removed from the intensity field, similar to the development in Section 16.8, the resulting modified P_1-approximation may be expected to give accurate solutions to equations (19.12) and (19.14) for many situations. To apply the method, we assume again that the remnant intensity can deviate only slightly from isotropic conditions or, from equation (16.31),

$$I_d(\mathbf{r}, \hat{\mathbf{s}}) \simeq \frac{1}{4\pi} \left[G_d(\mathbf{r}) + 3\mathbf{q}_d(\mathbf{r}) \cdot \hat{\mathbf{s}} \right]. \tag{19.16}$$

As in Section 16.5 we shall limit ourselves to linear-anisotropic scattering,

$$\Phi(\hat{\mathbf{s}}, \hat{\mathbf{s}}') = 1 + A_1 \hat{\mathbf{s}} \cdot \hat{\mathbf{s}}', \tag{19.17}$$

so that

$$\begin{aligned} S_c &= \frac{1}{4\pi} \int_{4\pi} I_c(\hat{\mathbf{s}}')(1 + A_1 \hat{\mathbf{s}} \cdot \hat{\mathbf{s}}')\, d\Omega' \\ &= \frac{1}{4\pi} (G_c + A_1 \mathbf{q}_c \cdot \hat{\mathbf{s}}) = \frac{1}{4\pi} [1 - \rho(\mathbf{r}_w)] q(\mathbf{r}_w)\, e^{-\tau_c} (1 + A_1 \hat{\mathbf{s}} \cdot \hat{\mathbf{s}}_c). \end{aligned} \tag{19.18}$$

Now, integrating equation (19.12) over all directions (zeroth moment), we obtain

$$\nabla_\tau \cdot \mathbf{q}_d = (1 - \omega)(4\pi I_b - G_d) + \omega G_c. \tag{19.19}$$

Similarly, integrating equation (19.12) after multiplication with $\hat{\mathbf{s}}$ and invoking equation (19.16), we obtain

$$\frac{1}{3} \nabla_\tau G_d = -\left(1 - \frac{A_1 \omega}{3}\right) \mathbf{q}_d + \frac{A_1 \omega}{3} \mathbf{q}_c. \tag{19.20}$$

As for the standard P_1-approximation, the necessary boundary conditions for this set of equations are found by demanding continuity of heat flux normal to the surface at the boundary, that is,

$$\mathbf{q}_d \cdot \hat{\mathbf{n}}(\mathbf{r}_w) = \int_{4\pi} I_d(\mathbf{r}_w, \hat{\mathbf{s}})\, \hat{\mathbf{n}} \cdot \hat{\mathbf{s}}\, d\Omega, \tag{19.21}$$

with $I_d(\mathbf{r}_w, \hat{\mathbf{s}})$ from equation (19.16) for incoming directions ($\hat{\mathbf{n}} \cdot \hat{\mathbf{s}} < 0$), and from equation (19.14) for outgoing directions ($\hat{\mathbf{n}} \cdot \hat{\mathbf{s}} > 0$). Calculating first the diffuse irradiation leads to

$$\begin{aligned} -H_d(\mathbf{r}_w) &= \int_{\hat{\mathbf{n}} \cdot \hat{\mathbf{s}} < 0} I_d(\mathbf{r}_w, \hat{\mathbf{s}})\, \hat{\mathbf{n}} \cdot \hat{\mathbf{s}}\, d\Omega = \frac{1}{4\pi} \int_0^{2\pi} \int_{\pi/2}^{\pi} (G_d + 3\mathbf{q}_d \cdot \hat{\mathbf{s}})\, \hat{\mathbf{n}} \cdot \hat{\mathbf{s}}\, d\Omega \\ &= \frac{1}{2} \int_{\pi/2}^{\pi} (G_d + 3\mathbf{q}_d \cdot \hat{\mathbf{n}} \cos\theta) \cos\theta \sin\theta\, d\theta = -\frac{G_d}{4} + \frac{\mathbf{q}_d \cdot \hat{\mathbf{n}}}{2}. \end{aligned} \tag{19.22}$$

Thus,

$$\mathbf{q}_d \cdot \hat{\mathbf{n}} = \epsilon \pi I_{bw} + \rho\, (H_c + H_d) - H_d,$$

or, after substituting equation (19.22),

$$\mathbf{r} = \mathbf{r}_w : \qquad 2\mathbf{q}_d \cdot \hat{\mathbf{n}} = \frac{\epsilon(4\pi I_{bw} - G_d) + 4(1 - \epsilon) H_c}{2 - \epsilon}. \tag{19.23}$$

The derivation of equations (19.19) and (19.20) is very similar to the development of the standard P_1-approximation, which has been given in some greater detail in Section 16.5.

Example 19.2. Find the solution to the previous example using the P_1-approximation.

Solution
As for the exact solution we find

$$G_c = q_s\, e^{-\tau/\mu_o}, \qquad \mathbf{q}_c = G_c \hat{\mathbf{s}}_o,$$

and we realize again that G_d and $\mathbf{q}_d = q_d \hat{\mathbf{k}}$ depend on τ (optical distance perpendicular to the layer) only. Thus, from equations (19.19) and (19.20) and their boundary conditions (19.23), we find that

$$\begin{aligned} \frac{dq_d}{d\tau} &= -(1-\omega)G_d + \omega G_c, \\ \frac{dG_d}{d\tau} &= -3q_d, \\ \tau = 0: \qquad & 2q_d = -G_d, \\ \tau = \tau_L: \qquad & -2q_d = -G_d. \end{aligned}$$

Since the solution procedure for this equation is different for $\omega = 1$ (as opposed to $\omega < 1$), and since we would like to compare the present results with exact ones shown in Fig. 19-4, we shall limit the rest of our discussion to $\omega = 1$. Then

$$\frac{dq_d}{d\tau} = q_s\, e^{-\tau/\mu_o}, \quad \text{or} \qquad q_d = -\mu_o q_s\, e^{-\tau/\mu_o} + C_1,$$

$$\frac{dG_d}{d\tau} = -3q_d, \quad \text{or} \qquad G_d = -3\mu_o^2 q_s\, e^{-\tau/\mu_o} - 3C_1\tau + C_2.$$

It follows from the boundary conditions that

$$\begin{aligned} \tau = 0: \qquad & 2C_1 + C_2 = (2+3\mu_o)\,\mu_o q_s, \\ \tau = \tau_L: \qquad & (2+3\tau_L)\,C_1 - C_2 = (2-3\mu_o)\,\mu_o q_s\, e^{-\tau/\mu_o}, \end{aligned}$$

or

$$\begin{aligned} C_1 &= \frac{2+3\mu_o + (2-3\mu_o)\,e^{-\tau_L/\mu_o}}{4+3\tau_L}\,\mu_o\, q_s, \\ q_d &= \left[\frac{2+3\mu_o + (2-3\mu_o)\,e^{-\tau_L/\mu_o}}{4+3\tau_L} - e^{-\tau/\mu_o}\right]\mu_o q_s. \end{aligned}$$

Finally,

$$\Psi = \frac{\mathbf{q}_c \cdot \hat{\mathbf{k}} + q_d}{q_s} = \frac{2+3\mu_o + (2-3\mu_o)\,e^{-\tau_L/\mu_o}}{4+3\tau_L}\,\mu_o,$$

which, as discussed in the previous example, is constant across the layer. This nondimensional heat flux is compared with the exact result in Fig. 19-4. It is seen that the P_1-approximation gives good accuracy for all cases shown in that figure.

Some two-dimensional examples for the P_1-approximation with collimated irradiation have been given by Modest and Tabanfar [47], comparing with exact results by Crosbie and Koewing [48] and Crosbie and Dougherty [10]. The accuracy of the P_1-approximation was found to be excellent in most cases, since it is generally applied to an "emitting" medium with cold boundaries. As expected, the accuracy of the P_1-approximation decreases if sharp gradients of the radiative source occur within the medium (e.g., a source resulting from scattering of a highly focused, penetrating laser beam).

19.4 SHORT-PULSED COLLIMATED IRRADIATION WITH TRANSIENT EFFECTS

If a laser pulse of extremely short duration, usually accompanied by strong temporal variation over the duration of the pulse, impinges on a medium, the transient term in the radiative transfer equation becomes of importance. Therefore, according to equation (10.20), equation (19.12) must be reformulated as

$$\frac{1}{\beta c}\frac{\partial I_d}{\partial t}(\mathbf{r},\hat{\mathbf{s}},t)+\frac{1}{\beta}\hat{\mathbf{s}}\cdot\nabla I_d(\mathbf{r},\hat{\mathbf{s}})=-I_d(\mathbf{r},\hat{\mathbf{s}})+\frac{\omega}{4\pi}\int_{4\pi} I_d(\mathbf{r},\hat{\mathbf{s}}')\,\Phi(\hat{\mathbf{s}},\hat{\mathbf{s}}')\,d\Omega' + (1-\omega)\,I_b(\mathbf{r})+\omega S_c(\mathbf{r},\hat{\mathbf{s}}), \quad (19.24)$$

in which the "diffuse intensity" I_d and the scattering source S_c are now functions of time as well as of location and direction. Furthermore, the remnant of the collimated irradiation, entering the medium at point $\mathbf{r}_w$, arrives at location $\mathbf{r}$ with a time delay of $s/c = |\mathbf{r}-\mathbf{r}_w|/c$. Therefore, equation (19.13) must be replaced by

$$S_c(\mathbf{r},\hat{\mathbf{s}},t)=\frac{1}{4\pi}\left[1-\rho(\mathbf{r}_w)\right]q_o(\mathbf{r}_w,t-s/c)\,e^{-\tau_c}\Phi(\hat{\mathbf{s}},\hat{\mathbf{s}}_c). \quad (19.25)$$

The boundary conditions remain essentially unchanged [except for the time delay in q_o in equation (19.15)]. Equation (19.24) is hyperbolic in nature, i.e., the signal (intensity) can travel (and change) with a signal velocity of c (the speed of light). This is also immediately obvious from the source term, equation (19.25). This set of equations has been solved, after transformation into an integral formulation, by Tan and Hsu [49] for a one-dimensional layer, and by Wu and Wu [27–30] for one-dimensional and two-dimensional, axisymmetric slabs. Hsu [50] used the Monte Carlo method of Chapter 21 to predict incident radiation and fluxes in a one-dimensional slab, while Guo and coworkers [24] employed the Monte Carlo method for a two-dimensional, axisymmetric field. The backward Monte Carlo scheme was applied by Lu and Hsu [51, 52] to predict one-dimensional slab reflectivities and transmissivities.

A number of approximate models based on the RTE solution methods presented in Chapters 15–17 have also been developed. Considering a one-dimensional slab with nonreflecting boundaries, Kumar and coworkers [21] extended the modified P_1-approximation to this case, and a little later Mitra and Kumar [23] added two-flux and discrete ordinates formulations. They noted that the signal velocity of the two-flux approximation is only $c/2$, while the P_1-approximation has a signal velocity of $c/\sqrt{3}$. As higher-order methods are used, either spherical harmonics, P_N, or discrete ordinates, S_N, the correct signal velocity, c, is approached. Noting this incorrect phase velocity of the P_1-approximation, Olson and colleagues [25] and Morel [26] modified the method into what they dubbed the $P_{1/3}$-approximation.

Several investigators [43, 53, 54] extended the regular discrete ordinates method (DOM) to transient problems, and Chai and coworkers [55–57] did so for the related finite volume method (FVM) as applied to one-, two-, and three-dimensional problems. Finally, Liu and coworkers [58–60] showed how a variant of the FVM, using discontinuous finite elements for spatial discretization, can be employed for transient calculations. Apparently, Liu and Hsu [60] have been the first to recognize that, because equation (19.24) is linear in time, solutions to arbitrary temporal pulse shapes (and pulse trains) can be found by superposition.

In all cases discussed above the medium was assumed to be nonemitting. A few studies have considered heating of the material and emission from it, assuming radiative equilibrium to hold, equation (10.74) [61, 62], and some included Fourier conduction, as well [61, 63], and even hyperbolic conduction [44].

Because of their simplicity and popularity, we will here briefly outline the development of, both, the P_1- and the $P_{1/3}$-approximations for a nonemitting medium.

P_1-Formulation

The starting point is now the augmented RTE, equation (19.24). After taking the zeroth and first moments, and again using the near-isotropy condition, equation (19.16), and the assumption of linear-anisotropic scattering, equation (19.17), the augmented P_1-equations (19.19) and (19.20) become

$$\frac{\partial G_d}{\partial t^*} + \nabla_\tau \cdot \mathbf{q}_d = (1-\omega)(4\pi I_b - G_d) + \omega G_c, \tag{19.26}$$

$$\frac{\partial \mathbf{q}_d}{\partial t^*} + \frac{1}{3}\nabla_\tau G_d = -\left(1 - \frac{A_1\omega}{3}\right)\mathbf{q}_d + \frac{A_1\omega}{3}\mathbf{q}_c, \tag{19.27}$$

where $t^* = \beta ct$ is a nondimensional time. These equations are, of course, identical to equations (19.19) and (19.20) except for the addition of a transient term. As for the exact formulation, the boundary conditions, equation (19.23), remain unchanged [again, except for the time delay in q_o in equation (19.15)]. Elimination of $\mathbf{q}_d$ from equations (19.26) and (19.27) results in a hyperbolic wave equation for G_d with a signal velocity of $c/\sqrt{3}$.

$P_{1/3}$-Formulation

Olson and coworkers [25] noticed that, if the transient term in equation (19.27) is multiplied by 1/3, the resulting set of equations has the correct propagation velocity c, while still reducing to the correct steady-state P_1-approximation. The so-called $P_{1/3}$-approximation is, therefore,

$$\frac{\partial G_d}{\partial t^*} + \nabla_\tau \cdot \mathbf{q}_d = (1-\omega)(4\pi I_b - G_d) + \omega G_c, \tag{19.28}$$

$$\frac{1}{3}\frac{\partial \mathbf{q}_d}{\partial t^*} + \frac{1}{3}\nabla_\tau G_d = -\left(1 - \frac{A_1\omega}{3}\right)\mathbf{q}_d + \frac{A_1\omega}{3}\mathbf{q}_c, \tag{19.29}$$

again subject to the boundary condition, equation (19.23). While the multiplication by the factor 1/3 appears arbitrary, one should keep in mind that equation (19.27) is already approximate (through the use of the near-isotropy condition, equation (19.16)), and thus can be augmented by a transient term to produce the desired result.

Example 19.3. Consider a cold medium of width L ($0 \le x \le L$) with refractive index $n = 1$, bounded by vacuum (resulting in nonreflecting interfaces). The medium absorbs, scatters isotropically, and is subjected to a square laser pulse at $x = 0$, according to

$$q_o(0,t) = q_o[H(t) - H(t-t_p)],$$

where t_p is the duration of the pulse and $H(t)$ is Heaviside's unit step function.[4] Determine the transmissivity of the slab as a function of time. (This is essentially the example problem carried out by Mitra and Kumar [23] and by Wu and Ou [31].)

Solution

For a nonemitting and isotropically scattering, one-dimensional medium, the equations for the P_1- and $P_{1/3}$-approximations reduce to

$$\frac{\partial G}{\partial t^*} + \frac{\partial q}{\partial \tau} = -(1-\omega)G + \omega G_c,$$

$$3a\frac{\partial q}{\partial t^*} + \frac{\partial G}{\partial \tau} = -3q,$$

where $a = 1$ for P_1 and $a = 1/3$ for $P_{1/3}$, and G and q have been normalized as $G = G_d/q_o$ and $q = q_d/q_o$. These two equations are subject to the initial and boundary conditions

$$t^* = 0: \quad G(0,\tau) = q(0,\tau) = 0,$$

$$\tau = 0: \quad -2q(t^*,0) = G(t^*,0),$$

$$\tau = \tau_L: \quad +2q(t^*,\tau_L) = G(t^*,\tau_L).$$

[4] For its definition see equation (11.103) in Section 11.9.

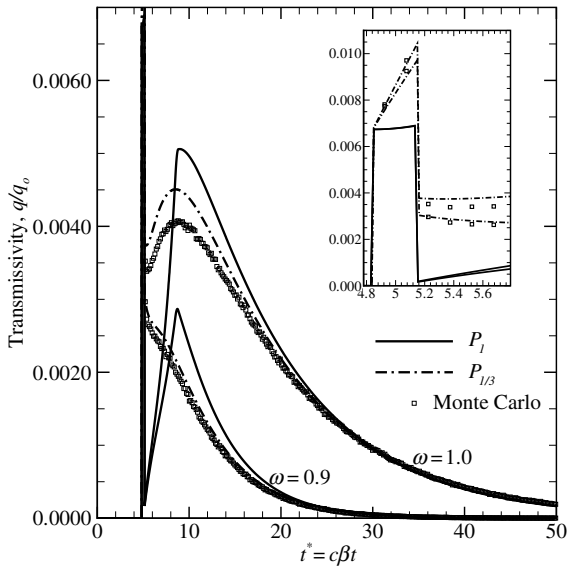

FIGURE 19-5
Transient transmissivity of an absorbing–scattering slab subjected to a collimated square laser pulse ($t_p^* = 0.3, \tau_L = 5$).

The normalized isotropic scattering source is immediately found from equations (19.25) and (19.18) for a nonreflecting boundary, as

$$G_c(t^*, \tau) = \left[H(t^* - \tau) - H^*(t^* - \tau - t_p^*)\right] e^{-\tau}.$$

The hyperbolic nature of this set of equations becomes obvious, if q is eliminated from them (by differentiating the first with respect to t^* and the second with respect to τ), leading to

$$\frac{\partial^2 G}{\partial t^{*2}} - \frac{1}{3a}\frac{\partial^2 G}{\partial \tau^2} + \left(1 - \omega + \frac{1}{a}\right)\frac{\partial G}{\partial t^*} + \frac{1-\omega}{a}G - \frac{\omega}{a}G_c - \omega\frac{\partial G_c}{\partial t^*} = 0,$$

which has a signal velocity of $1/\sqrt{3a}$ (nondimensional in terms of speed of light, c), as already indicated in the formulation for the P_a methods. Eliminating q also from the initial and boundary conditions gives

$$t^* = 0: \quad G(0,\tau) = \frac{\partial G}{\partial t^*}(0,\tau) = 0,$$

$$\tau = 0: \quad 3\left(G(t^*,0) + a\frac{\partial G}{\partial t^*}(t^*,0)\right) - 2\frac{\partial G}{\partial \tau}(t^*,0) = 0,$$

$$\tau = \tau_L: \quad 3\left(G(t^*,0) + a\frac{\partial G}{\partial t^*}(t^*,0)\right) + 2\frac{\partial G}{\partial \tau}(t^*,0) = 0.$$

This second-order hyperbolic equation is readily solved by the method of characteristics [64] along the characteristic lines $\tau = \pm t^*/\sqrt{3a}$, and this was done in the program `transPN` given in Appendix F. Some typical results for the temporal transmission rate, $[q_c(\tau_L) + q_d(\tau_L)]/q_o$, are shown in Fig. 19-5, for a slab with an optical thickness of $\tau_L = 5$ and a nondimensional pulse width $t_p^* = 0.3$ and are compared with results from a Monte Carlo simulation (see Problem 21.8). The transmissivity remains zero until $t^* = \tau_L$, since it takes the direct component that amount of time to traverse the layer. As is clearly visible in the inset, between $\tau_L < t^* < \tau_L + t_p^*$ the transmissivity is dominated by the direct component $q_c(\tau_L)/q_o$, while the scattered contribution builds up gradually and, for $\omega = 1$, reaches its maximum around $t^* \simeq 9$. It is apparent that the P_1-approximation, with its $c/\sqrt{3}$ signal velocity, woefully lags behind the true transmissivity, and later overshoots, while the $P_{1/3}$-approximation predicts the transient behavior rather accurately.

Wu and Ou [31] used a clipped Gaussian laser pulse (rather than the square pulse), and noted that the P_1-approximation produced an unphysical, secondary spike at $t^* = \sqrt{3}\tau_L$ (i.e., the time it takes radiation scattered at $\tau = 0$ to reach $\tau = \tau_L$ in a direct path), while the $P_{1/3}$-approximation

does not show this behavior. Apparently, this is due to the fact that, for a Gaussian profile, $\partial G_c/\partial t^* \neq 0$, which produces the secondary peak (this may be verified by running `transPN` with its preprogrammed Gaussian pulse).

Since the transient RTE is hyperbolic in nature, the method of characteristics is often used in numerical solutions (including `transPN`), in order to accurately capture the radiation wavefront. Katika and Pilon [65] introduced a modified (backward) characteristic method that gives better flexibility in time stepping. If hyperbolic equations are solved by conventional differencing, second-order time schemes are generally preferred. Olson [63, 66] has discussed several first- and second-order time stepping techniques for such methods.

References

1. Irvine, W. M.: "Multiple scattering by large particles II. Optically thick layers," *The Astrophysical Journal*, vol. 152, pp. 823–834, 1968.
2. Van de Hulst, H. C.: *Light Scattering by Small Particles*, John Wiley & Sons, New York, 1957, (also Dover Publications, New York, 1981).
3. Kubo, S.: "Effects of anisotropic scattering on steady one-dimensional radiative heat transfer through an absorbing–emitting medium," *J. Phys. Soc. Japan*, vol. 41, no. 3, pp. 894–898, 1976.
4. Armaly, B. F., and H. S. El-Baz: "Radiative transfer through an isotropically scattering finite medium: Approximate solution," *AIAA Journal*, vol. 15, no. 8, pp. 1180–1185, 1976.
5. Houf, W. G., and F. P. Incropera: "An assessment of techniques for predicting radiation transfer in aqueous media," *Journal of Quantitative Spectroscopy and Radiative Transfer*, vol. 23, pp. 101–115, 1980.
6. Smith, M. G.: "The transport equation with plane symmetry and isotropic scattering," *Proc. Camb. Phil. Soc.*, vol. 60, p. 909, 1964.
7. Hunt, G. E.: "The transport equation of radiative transfer with axial symmetry," *SIAM J. Appl. Math.*, vol. 16, no. 1, pp. 228–237, 1968.
8. Beckett, P., P. J. Foster, V. Huston, and R. L. Moss: "Radiative transfer for a cylindrical beam scattered isotropically," *Journal of Quantitative Spectroscopy and Radiative Transfer*, vol. 14, pp. 1115–1125, 1974.
9. Crosbie, A. L., and T. L. Linsenbardt: "Two-dimensional isotropic scattering in a semi-infinite medium," *Journal of Quantitative Spectroscopy and Radiative Transfer*, vol. 19, pp. 257–284, 1978.
10. Crosbie, A. L., and R. L. Dougherty: "Two-dimensional isotropic scattering in a semi-infinite cylindrical medium," *Journal of Quantitative Spectroscopy and Radiative Transfer*, vol. 20, pp. 151–173, 1978.
11. Crosbie, A. L., and R. L. Dougherty: "Two-dimensional linearly anisotropic scattering in a semi-infinite cylindrical medium exposed to a laser beam," *Journal of Quantitative Spectroscopy and Radiative Transfer*, vol. 28, no. 3, pp. 233–263, 1982.
12. Crosbie, A. L., and R. G. Schrenker: "Multiple scattering in a two-dimensional rectangular medium exposed to collimated radiation," *Journal of Quantitative Spectroscopy and Radiative Transfer*, vol. 33, no. 2, pp. 101–125, 1985.
13. Kim, T. K., and H. S. Lee: "Radiative transfer in two-dimensional anisotropic scattering media with collimated incidence," *Journal of Quantitative Spectroscopy and Radiative Transfer*, vol. 42, pp. 225–238, 1989.
14. Tan, H. P., L. Ruan, and T. W. Tong: "Temperature response in absorbing, isotropic scattering medium caused by laser pulse," *International Journal of Heat and Mass Transfer*, vol. 43, no. 2, pp. 311–320, 2000.
15. Lacroix, D., G. Jeandel, and C. Boudot: "Solution of the radiative transfer equation in an absorbing and scattering Nd:YAG laser-induced plume," *Journal of Applied Physics*, vol. 84, pp. 2443–2449, 1998.
16. Xu, X., and K. H. Song: "Radiative transfer between the pulsed laser and the target in the presence of laser-induced plasma," in *Transport Phenomena in Materials Processing and Manufacturing*, vol. HTD-336, ASME, pp. 9–16, 1996.
17. Xu, X., and K. H. Song: "Radiative transfer in pulsed-laser induced plasma," *ASME Journal of Heat Transfer*, vol. 119, no. 3, pp. 502–508, 1997.
18. El Ammouri, F., A. Soufiani, and J. Taine: "Analysis of laser beam deviation fluctuations in a turbulent non-isothermal flow and relevance to ϵ_θ," *International Journal of Heat and Mass Transfer*, vol. 38, no. 17, pp. 3135–3142, 1995.
19. Ben-Abdallah, P., V. Le Dez, D. Lemonnier, S. Fumeron, and A. Charette: "Inhomogeneous radiative model of refractive and dispersive semi-transparent stellar atmospheres," *Journal of Quantitative Spectroscopy and Radiative Transfer*, vol. 69, pp. 61–80, 2001.
20. Kumar, S., and K. Mitra: "Microscale aspects of thermal radiation transport and laser applications," in *Advances in Heat Transfer*, vol. 33, Academic Press, New York, pp. 187–294, 1999.
21. Kumar, S., K. Mitra, and Y. Yamada: "Hyperbolic damped-wave models for transient light-pulse propagation in scattering media," *Applied Optics*, vol. 35, no. 19, pp. 3372–3378, 1996.
22. Mitra, K., and S. Kumar: "Interaction of short pulse radiation with scattering media: Issues and transient radiative transfer formulation," in *Proceedings of the 11th International Heat Transfer Conference*, vol. 7, pp. 313–318, 1998.

23. Mitra, K., and S. Kumar: "Development and comparison of models for light-pulse transport through scattering absorbing media," *Applied Optics*, vol. 38, no. 1, pp. 188–196, 1999.
24. Guo, Z., J. Aber, B. A. Garetz, and S. Kumar: "Monte Carlo simulation and experiments of pulsed radiative transfer," *Journal of Quantitative Spectroscopy and Radiative Transfer*, vol. 73, pp. 159–168, 2002.
25. Olson, G. L., L. H. Auer, and M. L. Hall: "Diffusion, P_1, and other approximate forms of radiation transport," *Journal of Quantitative Spectroscopy and Radiative Transfer*, vol. 64, pp. 619–634, 2000.
26. Morel, J. E.: "Diffusion-limit asymptotics of the transport equation, the $P_{1/3}$ equations, and two flux-limited diffusion theories," *Journal of Quantitative Spectroscopy and Radiative Transfer*, vol. 65, pp. 769–778, 2000.
27. Wu, C. Y., and S. H. Wu: "Integral equation formulation for transient radiative transfer in an anisotropically scattering medium," *International Journal of Heat and Mass Transfer*, vol. 43, no. 11, pp. 2009–2020, 2000.
28. Wu, S. H., and C. Y. Wu: "Integral equation solutions for transient radiative transfer in nonhomogeneous anisotropically scattering media," *ASME Journal of Heat Transfer*, vol. 122, no. 4, pp. 818–822, 2000.
29. Wu, C. Y.: "Propagation of scattered radiation in a participating planar medium with pulse irradiation," *Journal of Quantitative Spectroscopy and Radiative Transfer*, vol. 64, pp. 537–548, 2000.
30. Wu, S. H., and C. Y. Wu: "Time-resolved spatial distribution of scattered radiative energy in a two-dimensional cylindrical medium with a large mean free path for scattering," *International Journal of Heat and Mass Transfer*, vol. 44, pp. 2611–2619, 2001.
31. Wu, C. Y., and N. R. Ou: "Differential approximations for transient radiative transfer through a participating medium exposed to collimated irradiation," *Journal of Quantitative Spectroscopy and Radiative Transfer*, vol. 73, pp. 111–120, 2002.
32. Sakami, M., K. Mitra, and P.-F. Hsu: "Analysis of light pulse transport through two-dimensional scattering and absorbing media," *Journal of Quantitative Spectroscopy and Radiative Transfer*, vol. 73, pp. 169–179, 2002.
33. Longtin, J. P., and C. L. Tien: "Saturable absorption during high-intensity laser heating of liquids," *ASME Journal of Heat Transfer*, vol. 118, no. 4, pp. 924–930, 1996.
34. Luk'yanchuk, B., N. Bityurin, S. Anisimov, N. Arnold, and D. Bäuerle: "The role of excited species in ultraviolet-laser materials ablation III: Non-stationary ablation of organic polymers," *Applied Physics A*, vol. 62, pp. 397–401, 1996.
35. Nikogosyan, D. N., A. A. Oraevsky, and V. I. Rupasov: "Two-photon ionization and dissociation of liquid water by powerful laser UV radiation," *Chemical Physics*, vol. 77, pp. 131–143, 1983.
36. Pèpin, C., D. Houde, H. Remita, T. Goulet, and J.-P. Jay-Gerin: "Evidence for resonance-enhanced multiphoton ionization of liquid water using 2-eV laser light: variation of hydrated electron absorbance with femtosecond pulse intensity," *Physical Review Letters*, vol. 69, pp. 3389–3392, 1992.
37. Longtin, J. P., and C. L. Tien: "Efficient laser heating of transparent liquids using multiphoton absorption," *International Journal of Heat and Mass Transfer*, vol. 40, no. 4, pp. 951–959, 1997.
38. Sauerbrey, R., and G. H. Pettit: "Theory for the etching of organic materials by ultraviolet laser pulses," *Applied Physics Letters*, vol. 55, no. 5, pp. 421–423, 1989.
39. Cain, S. R., F. C. Burns, C. E. Otis, and B. Braren: "Photothermal description of polymer ablation: absorption behavior and degradation time scales," *Journal of Applied Physics*, vol. 72, no. 11, pp. 5172–5178, 1992.
40. Bityurin, N., and A. Malyshev: "UV-laser ablation of absorbing dielectrics by ultra-short laser pulses," *Applied Surface Science*, vol. 127–129, pp. 199–205, 1998.
41. Sadoqi, M., S. Kumar, and Y. Yamada: "Photochemical and photothermal model for pulsed-laser ablation," *Journal of Thermophysics and Heat Transfer*, vol. 16, no. 2, pp. 193–199, 2002.
42. Guo, Z., and K. Kim: "Ultrafast-laser-radiation transfer in heterogeneous tissues with the discrete-ordinates method," *Applied Optics*, vol. 42, no. 16, pp. 2897–2905, 2003.
43. Trivedi, A., S. Basu, and K. Mitra: "Temporal analysis of reflected optical signals for short pulse laser interaction with nonhomogeneous tissue phantoms," *Journal of Quantitative Spectroscopy and Radiative Transfer*, vol. 93(1-3), pp. 337–348, 2005.
44. Jaunich, M., S. Raje, K. Kim, K. Mitra, and Z. Guo: "Bio-heat transfer analysis during short pulse laser irradiation of tissues," *International Journal of Heat and Mass Transfer*, vol. 51, pp. 5511–5521, 2008.
45. Duley, W. W.: *Laser Processing and Analysis of Materials*, Plenum Press, New York, 1983.
46. Bang, S. Y., and M. F. Modest: "Evaporative scribing with a moving CW laser—effects of multiple reflections and beam polarization," in *Proceedings of ICALEO '91, Laser Materials Processing*, vol. 74, San Jose, CA, pp. 288–304, 1992.
47. Modest, M. F., and S. Tabanfar: "A multi-dimensional differential approximation for absorbing/emitting anistropically scattering media with collimated irradiation," *Journal of Quantitative Spectroscopy and Radiative Transfer*, vol. 29, pp. 339–351, 1983.
48. Crosbie, A. L., and J. W. Koewing: "Two-dimensional radiative heat transfer in a planar layer bounded by nonisothermal walls," *AIAA Journal*, vol. 17, no. 2, pp. 196–203, 1979.
49. Tan, Z. M., and P.-F. Hsu: "An integral formulation of transient radiative transfer," *ASME Journal of Heat Transfer*, vol. 123, pp. 466–475, 2001.
50. Hsu, P.-F.: "Effects of multiple scattering and reflective boundary on the transient radiative transfer process," *International Journal of Thermal Sciences*, vol. 40, pp. 539–549, 2001.
51. Lu, X., and P.-F. Hsu: "Reverse Monte Carlo method for transient radiative transfer in participating media," *ASME Journal of Heat Transfer*, vol. 126(4), pp. 621–627, 2004.

52. Lu, X., and P.-F. Hsu: "Reverse Monte Carlo simulations of light pulse propagation in nonhomogeneous media," *Journal of Quantitative Spectroscopy and Radiative Transfer*, vol. 93(1-3), pp. 349–367, 2005.
53. Guo, Z., and S. Kumar: "Three-dimensional discrete ordinates method in transient radiative transfer," *Journal of Thermophysics and Heat Transfer*, vol. 16, no. 3, pp. 289–296, 2002.
54. Kim, K., and Z. Guo: "Ultrafast radiation heat transfer in laser tissue welding and soldering," *Numerical Heat Transfer – Part A: Applications*, vol. 46, no. 1, pp. 23–40, 2004.
55. Chai, J. C.: "One-dimensional transient radiation heat transfer modeling using a finite-volume method," *Numerical Heat Transfer – Part B: Fundamentals*, vol. 44, pp. 1–22, 2003.
56. Chai, J. C.: "Transient radiative transfer in irregular two-dimensional geometries," *Journal of Quantitative Spectroscopy and Radiative Transfer*, vol. 84, pp. 281–294, 2004.
57. Chai, J. C., P.-F. Hsu, and Y. C. Lam: "Three-dimensional transient radiative transfer modeling using the finite-volume method," *Journal of Quantitative Spectroscopy and Radiative Transfer*, vol. 86(3), pp. 299–313, 2004.
58. Liu, L. H., and L. J. Liu: "Discontinuous finite element approach for transient radiative transfer equation," *ASME Journal of Heat Transfer*, vol. 129(8), pp. 1069–1074, 2007.
59. Liu, L. H., and P.-F. Hsu: "Analysis of transient radiative transfer in semitransparent graded index medium," *Journal of Quantitative Spectroscopy and Radiative Transfer*, vol. 105, no. 3, pp. 357–376, 2007.
60. Liu, L. H., and P.-F. Hsu: "Time shift and superposition method for solving transient radiative transfer equation," *Journal of Quantitative Spectroscopy and Radiative Transfer*, vol. 109, no. 7, pp. 1297–1308, 2008.
61. Olson, G. L.: "Gray radiation transport in multi-dimensional stochastic binary media with material temperature coupling," *Journal of Quantitative Spectroscopy and Radiative Transfer*, vol. 104, no. 1, pp. 86–98, 2007.
62. Kim, M. Y., S. Menon, and S. W. Baek: "On the transient radiative transfer in a one-dimensional planar medium subjected to radiative equilibrium," *International Journal of Heat and Mass Transfer*, vol. 53, pp. 5682–5691, 2010.
63. Olson, G. L.: "Second-order time evolution of p_n equations for radiation transport," *Journal of Computational Physics*, vol. 228, pp. 3072–3083, 2009.
64. Ferziger, J. H.: *Numerical Methods for Engineering Application*, 2nd ed., John Wiley & Sons, New York, 1981.
65. Katika, K. M., and L. Pilon: "Modified method of characteristics in transient radiation transfer," *Journal of Quantitative Spectroscopy and Radiative Transfer*, vol. 98, no. 2, pp. 220–237, 2006.
66. Olson, G. L.: "Efficient solution of multi-dimensional flux-limited nonequilibrium radiation diffusion coupled to material conduction with second-order time discretization," *Journal of Computational Physics*, vol. 226, pp. 1181–1195, 2007.

Problems

19.1 A semi-infinite, gray, isotropically scattering medium, originally at zero temperature, is subjected to collimated irradiation with a constant flux q_o normal to its nonreflecting surface. Set up the integral relationships governing steady-state temperature and radiative heat flux within the medium, assuming radiative equilibrium.

19.2 In a greenhouse a layer of water (thickness $L = 5\,\text{cm}$) is resting on top of a black substrate. The water is loaded with growing organisms that scatter light isotropically but do not absorb ($\sigma_s = 0.2\,\text{cm}^{-1}$). The water layer is illuminated by two long growth-enhancing lights, fitted with reflector shields that make the light essentially parallel, as shown in the sketch, each light delivering a heat flux of $q_l = 100\,\text{W/m}^2$ (per unit area normal to the light rays). Using the exact method, calculate energy generated within the water and the radiative heat flux absorbed by the black surface in the zone between the lights, where the heat transfer is essentially one-dimensional. Emission from the water and substrate are negligible.
Hint: Use Figs. 3-16 and 19-4.

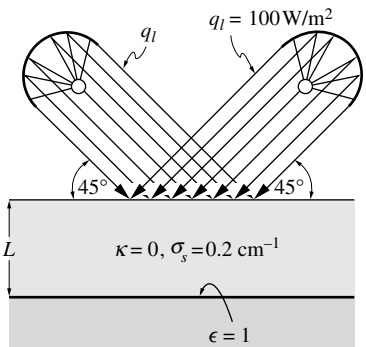

19.3 Reconsider the medium described in Example 19.1. Rather than being bounded by a cold black surface at the bottom, the layer is now exposed to the nonparticipating gas as well as to solar irradiation (using mirrors) on both sides. Determine radiative heat flux and its divergence within the layer in terms of the function $\Phi(\tau_L, \omega, \mu_o, \tau)$ given in Example 19.1.

19.4 Solve Problem 19.1 using the P_1-approximation.

19.5 The starship Enterprise is hitting a Klingon cruiser with its phaser gun. The armament of the cruiser is a partially reflecting material that, after some irradiation, partly evaporates, forming a protective gas layer above the surface. Assuming that the surface is at evaporation temperature T_{ev} and has an emittance ϵ, and that the gas has an absorption coefficient κ_g and a thickness L, determine the

fraction of the heat flux that hits the Klingon ship. Under these conditions you may assume the effects of conduction and convection to be negligible (but not reradiation from the gas). Use the P_1-approximation.

19.6 Reconsider Problem 19.5. After further irradiation, the surface material starts to disintegrate, spewing particulate material into the gas layer. If we make the assumption that the debris has an absorption coefficient κ_p and (isotropic) scattering coefficient σ_{sp}, how does this modify the surface irradiation?

19.7 Consider a semi-infinite gray medium with a nonreflecting surface. The medium is cold, and absorbs (absorption coefficient κ) and scatters isotropically (scattering coefficient σ_s). Collimated radiation obeying the relation

$$\mathbf{q}_c = q_o(1 - \cos\alpha\tau_x)\hat{\mathbf{k}}$$

shines normally onto the medium as shown below. Determine the reflectivity of the medium (i.e., the fraction of the irradiation leaving the interface in the opposite direction), using the P_1-approximation. Hint: To solve the two-dimensional governing equation, set $G_d(\tau_x, \tau_z) = G_1(\tau_z) + G_2(\tau_z)\cos\alpha\tau_x$.
This problem is a special case of solutions given by Crosbie and Koewing [48] (exact) and Modest and Tabanfar [47] (P_1).

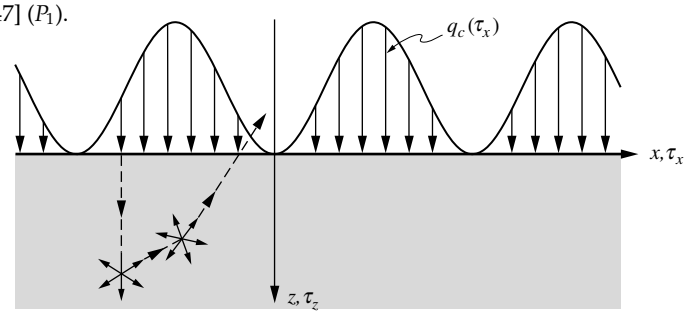

19.8 Reconsider Problem 19.2 for lights not fitted with reflector shields as depicted in the adjacent sketch. Assuming that the figure shows only two of many equally spaced lights (i.e., using symmetry), set up the solution for the radiative heat flux, using the P_1-approximation. Each light outputs a total of 100 W per meter length. Since this is a two-dimensional problem it will be sufficient to reduce the problem to the solution of a two-dimensional partial differential equation with stated boundary conditions.

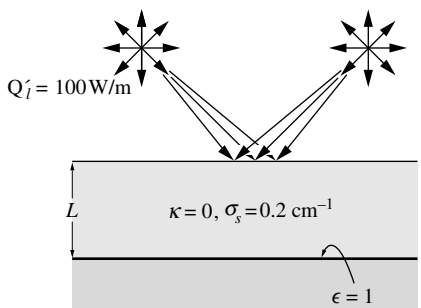

19.9 A slab of constant thickness L consisting of an absorbing and linear-anisotropically scattering medium, is subjected to collimated laser irradiation with a Gaussian flux profile $q_o(r) = (2\dot{Q}/\pi w^2)\, e^{-2(r/w)^2}$ normal to its nonreflecting surface, where r is radial distance from the beam center, w is the so-called "$1/e^2$-beam radius" and Q is total laser power (in W). Assuming the temperature of the medium to be moderate, emission can generally be neglected as compared to the laser flux. Show that this problem can be solved by the modified P_1-approximation, using subroutine `P1sor` and/or program `P1-2D` of Appendix F. Then determine the reflectivity of the medium (i.e., the fraction of the irradiation leaving the interface in the opposite direction), as a function of radius r, for a purely isotropically scattering medium with $\sigma_s = 5\,\text{cm}^{-1}$, $L = 1$ cm, and $w = 100\,\mu$m.

19.10 Repeat Example 19.3 for a clipped Gaussian laser pulse as considered by Wu and Ou [31], using program `transPN` of Appendix F.

19.11 Consider a cold medium of width L ($0 \le x \le L$) with refractive index $n = 1$, bounded by vacuum (resulting in nonreflecting interfaces). The medium absorbs, scatters isotropically, and is subjected to a CW ("continuous wave," or constant) laser pulse at $x = 0$ and starting at time $t = 0$, according to

$$q_o(0, t) = q_o H(t),$$

where $H(t)$ is Heaviside's unit step function. Determine the reflectivity and transmissivity of the slab as a function of time until steady state is achieved. Use program `transPN` of Appendix F.